

Reduced fluid modelling of shattered pellet injection in ASDEX Upgrade

P. Halldestam¹, P. Heinrich¹, G. Papp¹, M. Hoppe², M. Hölzl¹, I. Pusztai³, O. Vallhagen³, R. Fischer¹,
F. Jenko¹, the ASDEX Upgrade Team^a, and the EUROfusion Tokamak Exploitation Team^b

¹Max Planck Institute for Plasma Physics, Garching, Germany

²Department of Electrical Engineering, Royal Institute of Technology, Stockholm, Sweden

³Department of Physics, Chalmers University of Technology, Göteborg, Sweden

^aSee the author list of [H. Zohm et al. 2024 Nucl. Fusion](#)

^bSee the author list of [E. Joffrin et al. 2024 Nucl. Fusion](#)

Introduction One of the main issues threatening the success of future reactor-scale tokamaks are disruptions. It is the sudden loss of confinement where the plasma rapidly dissipates a large portion of its energy content onto the first wall, exposing the device to excessive mechanical stresses, heat loads, and can lead to the formation of a runaway electron beam. Unmitigated disruptions could potentially cause severe damage to the device and thus, modelling such events is crucial for being able to assess the effectiveness of various mitigation techniques. The ITER baseline disruption mitigation system will be based on shattered pellet injection (SPI) due to its ability to rapidly inject material into the plasma to thermally radiate its stored energy, reduce electromagnetic loads on surrounding conducting structures, and to inhibit the generation of runaway electrons. In support of its development, a highly flexible SPI system was installed at the ASDEX Upgrade tokamak (AUG) to investigate the impact of different fragment size and velocity distributions on the disruption dynamics [1].

In this contribution, a one-dimensional fluid model of the plasma was applied using the DREAM code [2], which is used to compare with AUG experiments the evolution of the plasma current and the fraction of the initial energy content that is dissipated as radiation. The plume of fragments is generated by sampling fragment size and velocity distributions that depend on various injection parameters, such as the speed of injection. The goal of this work is both to validate with experiment and to assess the impact that statistical variation in the fragment distributions has on the resulting disruption dynamics.

Random sampling of fragments The generation of the fragment plume is performed in two steps: a rejection sampling of fragment sizes, utilising an analytical distribution function for the characteristic fragment size following the pellet break-up [3, 4]; and then assigning velocities to the individual fragments. The fragment size probability distribution depends on the injection speed, shattering angle and pellet composition – here being a mixture of deuterium and neon. It

derives from a statistics based model for the shattering of brittle materials [3], which was correlated with the relevant SPI parameters in a comparison to experimentally measured fragment size distributions [4]. Fragments are sampled from this distribution in sequence until the total volume of all fragments exceeds the pellet volume. In doing so, the total number of fragments will depend on the specific random seed used during the sampling process.

In the second step, fragment speeds and directions are sampled independently from one another. The speeds are sampled from a normal distribution, where the mean fragment speed $\langle v_{\text{frag}} \rangle$ is assumed to be given by the average of the injection speed v_{inj} and its component parallel to the shattering surface at an angle of $\theta_s = 25^\circ$, i.e. $\langle v_{\text{frag}} \rangle = v_{\text{inj}}(1 + \cos \theta_s)/2$, and the spread in speed is assumed to be $\Delta v_{\text{frag}}/\langle v_{\text{frag}} \rangle = 20\%$ [5]. Finally, each fragment is assigned a direction in which it traverses through the plasma, which is sampled uniformly from the unit sphere within a cone with an opening angle of 20° .

Simulation setup To emulate the effect of the stochastisation of the magnetic field that causes the thermal energy to subsequently quench, an enhanced radial transport of heat, particles and poloidal magnetic flux is applied as the electron temperature reaches below 10eV within the resonant $q = 2$ surface. In practice, this is done by increasing a number of transport coefficients to some maximum value that exponentially decays over a timescale of 1 ms. This is relevant in three equations that are solved with the DREAM code, one of which is a modified version of Faraday's law of induction

$$\frac{\partial \psi_p}{\partial t} = -V_{\text{loop}} + \frac{\partial}{\partial \psi_t} \left[\psi_t \mu_0 \Lambda(t) \frac{\partial j_{\parallel}}{\partial \psi_t B} \right]. \quad (1)$$

Together with Ampères' law, equation (1) governs the evolution of the plasma current. It includes a hyperresistive term that acts to relax the current density while conserving the helicity content of the plasma [6]. This results in a brief spike in the plasma current before it subsequently decays, and by setting $\Lambda_{\text{max}} = 10^{-5} \text{ Wb}^2\text{m/s}$, we observe similar magnitudes in the current spike as seen in experiment. The electron thermal energy is evolved by an energy balance equation

$$\frac{3}{2} \frac{\partial n_e T_e}{\partial t} = \sigma_{\parallel} E_{\parallel}^2 - P_{\text{rad}} + P_{\text{col}} + \frac{1}{V'} \frac{\partial}{\partial r} \left[\frac{3n_e}{2} V' \chi_e(t) \frac{\partial T_e}{\partial r} \right], \quad (2)$$

which includes Ohmic heating, radiative cooling and collisional heat exchange with other particle species present in the plasma, and a diffusive transport, for which we set $\chi_{e,\text{max}} = 10^2 \text{ m}^2/\text{s}$ – its order of magnitude motivated by previous ASDEX Upgrade disruption simulations with

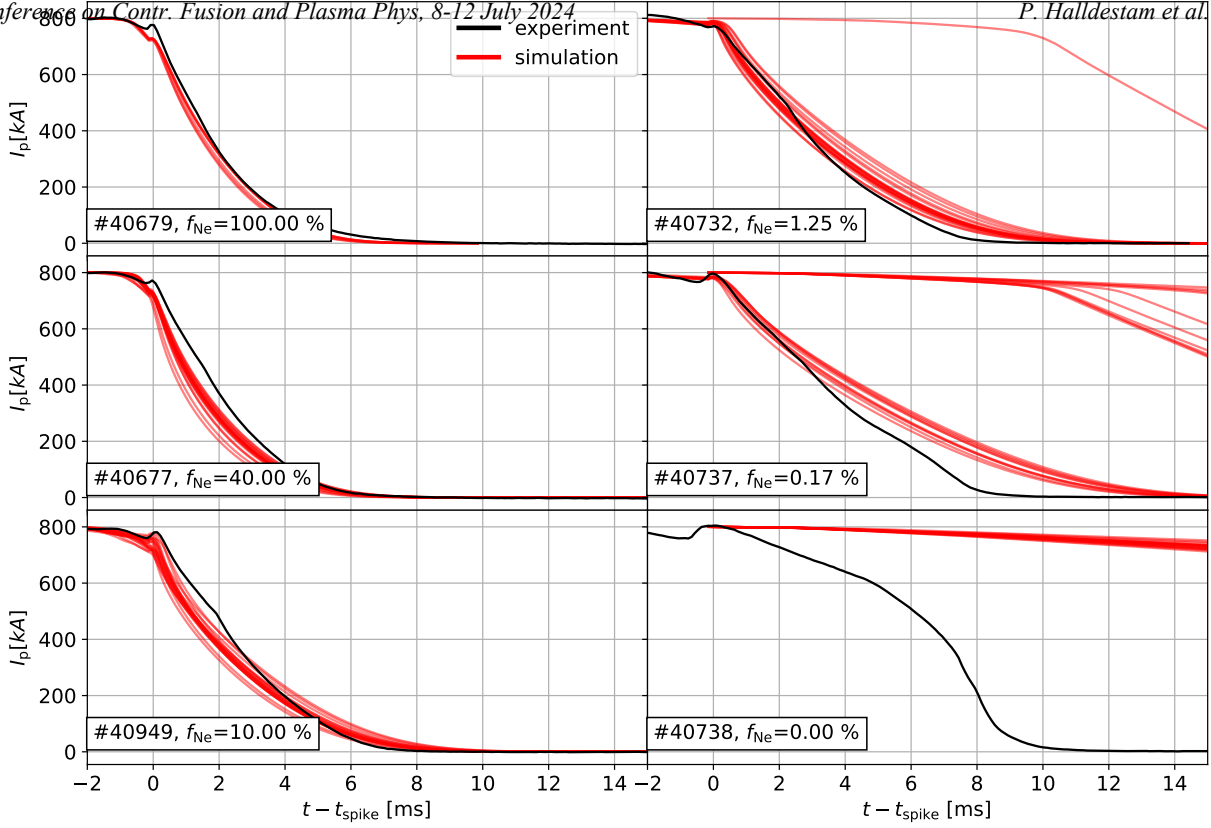


Figure 1: Comparison of the plasma current evolution for varying contents of injected neon in experiment measured data (black) and simulations (red). Each simulation is run 20 times using different random seeds while sampling fragments.

ASTRA [7]. Each ion charge state is evolved according to the rate equation

$$\frac{\partial n_i^{(j)}}{\partial t} = \frac{\partial n_i^{(j)}}{\partial t} \Big|_{\text{ionis}} + \frac{\partial n_i^{(j)}}{\partial t} \Big|_{\text{SPI}} + \frac{1}{V'} \frac{\partial}{\partial r} V' \left[A_i(t) n_i^{(j)} + D_i(t) \frac{\partial n_i^{(j)}}{\partial r} \right], \quad (3)$$

where the first term denote changes due to ionisation and recombination, the second is material deposited by the fragments as they ablate (plasmoid drifts are neglected). The last term describes advective and diffusive particle transport that is set equal across all ion species to be $A_{i,\text{max}} = -10^2 \text{ m/s}$ and $D_{i,\text{max}} = 10^2 \text{ m}^2/\text{s}$ [7].

Neon fraction dependence compared with experiment Each simulation uses initial conditions from the representative AUG shot #40655, for which kinetic profiles and magnetic equilibrium data is available by the reconstruction framework IDA [8]. Only the injection parameters are modified between the various shots, mainly the fraction of neon f_{Ne} in the pellet. To assess the statistical variations when sampling the fragments, each simulation is run 20 times with varying random seeds.

In figure 1, we compare simulations with six AUG shots where different amounts of neon is injected. The other injection parameters were kept roughly constant across all shots with $v_{inj} \approx 300$ m/s, and with pellet diameters $D = 8$ mm and lengths $L \approx 10$ mm. Note that the transport event is not always triggered for low f_{Ne} , whereas for the pure deuterium case this never occurs. This points to some missing physics in our model, possibly due to the omission of background impurities, e.g. tungsten.

For the same set of shots, we also compare the fraction of radiated energy f_{rad} with experimental estimates [9]. f_{rad} is the fraction of the initial total energy that gets dissipated as radiation during the duration of the disruption, and is a metric of the mitigation effectiveness. Figure 2 shows how simulations agree well with experiment in both magnitude and scaling in f_{Ne} , except for pure deuterium pellets, where f_{rad} is underestimated in our simulations. Again, this could possibly be due to the lack of background impurities in the current simulation setup. Including a small amount of tungsten in coronal equilibrium at the start of the simulation would introduce an additional channel for radiative losses, which could yield higher f_{rad} for trace amounts of neon. It could also conceivably cause an earlier trigger for the transport event, effectively decreasing f_{rad} for the higher neon contents. This is something we intend to investigate in the future.

References

- [1] M. DIBON ET AL. Review of Scientific Instruments, **94** (4):043504 (2023).
- [2] M. HOPPE ET AL. Computer Physics Communications, **268**:108098 (2021).
- [3] P. PARKS. General Atomics technical report, **GA (A28352)** (2016).
- [4] T. E. GEBHART ET AL. IEEE Transactions on Plasma Science, **48** (6):1598 (2020).
- [5] T. PEHERSTORFER. arXiv preprint, [arXiv:2209.01024](https://arxiv.org/abs/2209.01024) (2022).
- [6] A. H. BOOZER. Journal of Plasma Physics, **35**:133–139 (1986).
- [7] O. LINDER ET AL. Nuclear Fusion, **60** (9):096031 (2020).
- [8] R. FISCHER ET AL. Fusion Science and Technology, **58** (2):675 (2010).
- [9] P. HEINRICH ET AL. Nuclear Fusion paper in preparation.

This work has been carried out within the framework of the EUROfusion Consortium, funded by the European Union via the Euratom Research and Training Programme (Grant Agreement No 101052200 — EUROfusion). Views and opinions expressed are however those of the author(s) only and do not necessarily reflect those of the European Union or the European Commission. Neither the European Union nor the European Commission can be held responsible for them.

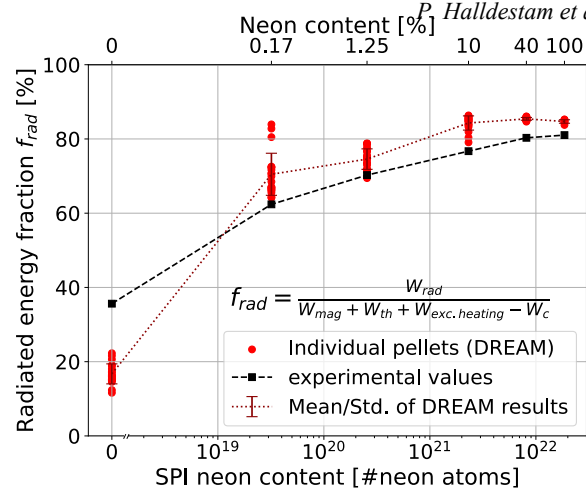


Figure 2: Radiated energy fraction f_{rad} from simulations (red) and experimental estimates (black) [9] as function of the amount of injected neon f_{Ne} .